IOPscience iopscience.iop.org

Home Search Collections Journals About Contact us My IOPscience

Determination of the Young's modulus of pulsed laser deposited epitaxial PZT thin films

This article has been downloaded from IOPscience. Please scroll down to see the full text article.

2011 J. Micromech. Microeng. 21 074008

(http://iopscience.iop.org/0960-1317/21/7/074008)

View the table of contents for this issue, or go to the journal homepage for more

Download details:
IP Address: 130.89.195.184
The article was downloaded on 23/06/2011 at 11:58

Please note that terms and conditions apply.

IOP Publishing — Journal of Micromechanics and Microengineering

J. Micromech. Microeng. **21** (2011) 074008 (7pp) doi:10.1088/0960-1317/21/7/074008

Determination of the Young's modulus of pulsed laser deposited epitaxial PZT thin films

H Nazeer[1], M D Nguyen[2], L A Woldering[1], L Abelmann[1], G Rijnders[2] and M C Elwenspoek[1,3]

[1] Transducers Science and Technology (TST), MESA+ Institute for Nanotechnology, University of Twente, PO Box 217, 7500 AE, Enschede, The Netherlands
[2] Inorganic Materials Science (IMS), MESA+ Institute for Nanotechnology, University of Twente, PO Box 217, 7500 AE, Enschede, The Netherlands
[3] FRIAS, Albert-Ludwigs University, Albertstr. 19, 79104 Freiburg, Germany

E-mail: h.nazeer@utwente.nl

Received 23 December 2010, in final form 13 April 2011
Published 22 June 2011
Online at stacks.iop.org/JMM/21/074008

Abstract
We determined the Young's modulus of pulsed laser deposited epitaxially grown $PbZr_{0.52}Ti_{0.48}O_3$ (PZT) thin films on microcantilevers by measuring the difference in cantilever resonance frequency before and after deposition. By carefully optimizing the accuracy of this technique, we were able to show that the Young's modulus of PZT thin films deposited on silicon is dependent on the in-plane orientation, by using cantilevers oriented along the ⟨1 1 0⟩ and ⟨1 0 0⟩ silicon directions. Deposition of thin films on cantilevers affects their flexural rigidity and increases their mass, which results in a change in the resonance frequency. An analytical relation was developed to determine the effective Young's modulus of the PZT thin films from the shift in the resonance frequency of the cantilevers, measured both before and after the deposition. In addition, the appropriate effective Young's modulus valid for our cantilevers' dimensions was used in the calculations that were determined by a combined analytical and finite-element (FE) simulations approach. We took extra care to eliminate the errors in the determination of the effective Young's modulus of the PZT thin film, by accurately determining the dimensions of the cantilevers and by measuring many cantilevers of different lengths. Over-etching during the release of cantilevers from the handle wafer caused an undercut. Since this undercut cannot be avoided, the effective length was determined and used in the calculations. The Young's modulus of PZT, deposited by pulsed laser deposition, was determined to be 103.0 GPa with a standard error of ± 1.4 GPa for the ⟨1 1 0⟩ crystal direction of silicon. For the ⟨1 0 0⟩ silicon direction, we measured 95.2 GPa with a standard error of ± 2.0 GPa.

(Some figures in this article are in colour only in the electronic version)

1. Introduction

In the micro-electromechanical systems (MEMS) industry, there is considerable interest in highly sensitive sensors and powerful actuators. To this end, $PbZr_{0.52}Ti_{0.48}O_3$ (PZT) is widely used for both piezoelectric actuation and sensing purposes. Printer manufacturers are, for instance, trying to incorporate PZT as an active device layer in inkjet printheads [1]. It is also a preferred choice for robotics applications [2], biosensors [3], and probe-based data storage devices [4] because of its high piezoelectric and ferroelectric properties. To support the use of this material in MEMS applications, information is needed on the mechanical properties in the thin film domain, certainly since these properties can differ from

 © 2011 IOP Publishing Ltd Printed in the UK & the USA

those of bulk materials [5]. Moreover, a large variation in the values of the PZT thin film's Young's modulus was published in the literature; for instance, in [6], the range was mentioned from 37 to 400 GPa.

PZT films can be deposited by processes like sol–gel [7], sputter [8] and pulsed laser deposition (PLD) [9]. Recently, excellent ferroelectric properties have been reported on PZT deposited by PLD [9]. However, accurate determination of the mechanical properties of PZT is being hampered by the fact that up to now only mm-square areas can be deposited uniformly using PLD. Mechanical characterization using full wafer techniques can therefore not be applied. Micrometer sized measurement devices provide a solution to this limitation. Many micro-sized structures such as cantilevers, membranes and bridges have been employed as test structures for determining the mechanical properties of thin films [10–12]. In particular, cantilevers are among the most widely used test structures for this purpose [13, 14]. We devised a method to accurately determine the effective Young's modulus of the PZT thin film by using the shift in the resonance frequency of microcantilevers before and after deposition of the thin film of PZT. Our demonstrated technique yields results with much higher accuracy compared to the similar methods reported in the literature [15, 16].

Accurate determination of the effective Young's modulus of PZT thin films from this resonance frequency method relies on the use of the appropriate effective Young's modulus of the cantilever material [17]. Since the epitaxial growth of the PZT by PLD on single crystal silicon might lead to in-plane anisotropy in Young's modulus [18], cantilevers oriented along the ⟨1 1 0⟩ and ⟨1 0 0⟩ crystal directions of silicon were analyzed. This analysis is discussed in section 2. In section 3, the fabrication of silicon cantilevers and the deposition of PZT thin films by PLD are explained. The determination of the effective Young's modulus of PZT depends on precise information about the geometrical dimensions of the cantilevers. In calculations, any uncertainty in these geometrical dimensions will propagate to the uncertainty in the final value of the Young's modulus of the PZT thin film. Therefore, the precise measurement of the thickness of cantilevers is an important parameter that reduces the uncertainty in the final result. This measurement is discussed in section 4. We observed an undesired undercut, which results from the deep reactive ion etching (DRIE) process that is used for the release of the cantilevers from the handle wafer. This undercut increases the effective length of the cantilevers [19, 20]. The effect of the undercut is incorporated in the calculation of the resonance frequency of cantilevers [21]. In section 4, we also present the orientation of the PZT and resonance frequency measurements of the PZT deposited cantilevers. Finally, in section 5, the Young's modulus of the PZT thin film deposited by PLD was determined using the effective length and appropriate effective Young's modulus relation valid for our cantilever dimensions.

2. Theory

2.1. Analytical relation for the resonance frequency of cantilevers

The resonance frequency of a cantilever without PZT is calculated by using the analytical relation [22]

$$f_n = \frac{C_n^2 t_s}{2\pi L^2}\sqrt{\frac{E_s^*}{12\rho}} \quad , \tag{1}$$

where f_n is the resonance frequency, C_n is a constant which depends on the vibration mode n, $C_0 = 1.875$ for the fundamental resonance frequency (f_0), E_s^* is the effective Young's modulus, ρ is the density of silicon [23], t_s is the thickness and L is the length of the cantilevers. The best approximation for the effective Young's modulus is required to calculate the resonance frequency of cantilevers. However, single crystal silicon is elastically anisotropic. Therefore, the effective Young's modulus of silicon is different for different crystal orientations. Consequently, the resonance frequencies of the cantilevers depend on their orientation with regard to the crystal lattice.

Equation (1) is a two-dimensional approximation. The third dimension is taken into account in the effective Young's modulus, which depends on the width of the cantilever. If the width is much larger than the length, the strain along that direction is zero. In this case, for very thin cantilevers and isotropic materials we can use the plate modulus $E/(1-\nu^2)$ as an approximation for the effective Young's modulus E^* [24], where E and ν are Young's modulus and Poisson's ratio, respectively. With reducing width, the stress in that direction is relaxed and the effective Young's modulus decreases to E for a width much smaller than the cantilever length. In our situation, the cantilever width is in the same order as the length. Moreover, single crystal silicon is anisotropic [25], so the two-dimensional situation was checked by finite-element (FE) calculations. We found that for cantilevers aligned parallel to the ⟨1 1 0⟩ and ⟨1 0 0⟩ crystal directions of the silicon crystal lattice, used in this study, the Young's modulus E itself and not the plate modulus $E/(1-\nu^2)$ is the best approximation [21].

2.2. Analytical model for the Young's modulus of PZT

The addition of PZT thin films on cantilevers affects their flexural rigidity and increases their mass. Both effects result in a change in the resonance frequency of the cantilevers. The effective Young's modulus of the PZT thin film is calculated using the resonance frequency both before and after deposition of the PZT thin film. We developed an analytical relation for the determination of Young's modulus of PZT as described in equation (2). The equation is based on a shift of the neutral axis and on the assumptions that the cantilever has a

uniform cross section, and that the cantilever deflection is small [22, 26]:

$$E_f^* = \frac{1}{t_f^3}\Bigg[6(t_s\rho_s + t_f\rho_f)B - 2E_s^* t_s^3 - 3t_f E_s^* t_s^2 - 2E_s^* t_s t_f^2 + 2\sqrt{\begin{array}{l} E_s^{*2} t_s^2 t_f^4 + 3E_s^{*2} t_s^3 t_f^3 + (4E_s^{*2} t_s^4 - 3AB)t_f^2 + \\ (3E_s^{*2} t_s^5 - 9ABt_s)t_f + E_s^{*2} t_s^6 - 6ABt_s^2 + \\ 9(t_s\rho_s + t_f\rho_f)^2 B^2 \end{array}}\Bigg], \quad (2)$$

where

$$A = E_s^* t_s (t_s\rho_s + t_f\rho_f),$$

and

$$B = \left(\sqrt{\frac{E_s^* t_s^3}{12 t_s \rho_s}} - 0.568\pi\Delta f_0 L^2\right)^2.$$

The symbols E^*, t, L and ρ are the effective Young's modulus, thickness, length and density, respectively. Subscripts 's' and 'f' denote the silicon and PZT thin film. Δf_0 is the difference in the fundamental resonance frequency of the cantilever before and after the deposition of PZT. By taking this difference, any potential uncertainties in the thickness of the cantilever can be eliminated and a more accurate result is obtained [12].

2.3. Analysis of uncertainties

Any uncertainty in measurement of the geometrical dimensions, frequency and physical parameters will affect the final calculated value of the Young's modulus of the PZT thin film. The uncertainty in Young's modulus of the thin film was calculated using the equation.

$$\frac{\Delta E_{f^*}}{E_{f^*}} = \frac{\partial E_f}{\partial x}\left[\frac{x}{E_f}\right]\left[\frac{\Delta x}{x}\right], \quad (3)$$

where x is any of the parameters L, t_s, t_f or ρ_f used on the right-hand side of equation (2). The cumulative error in the value of the effective Young's modulus of the PZT thin film is then calculated by the root mean square of the errors [27] calculated by using equation (3).

3. Fabrication

3.1. Fabrication of silicon cantilevers

A dedicated silicon on insulator (SOI)/MEMS fabrication process was used to fabricate 3 μm thick silicon cantilevers. The cantilevers are designed such that their length varies from 250 to 350 μm in steps of 10 μm, with a fixed width of 30 μm. Cantilevers were fabricated on the front side of (0 0 1) single crystal SOI wafers with the sequence as detailed in figure 1. A double side polished SOI wafer with a 3 μm thick device layer and a 500 nm thick SiO_2 buried oxide (BOX) layer was selected (*a*); the BOX serves as an etch stop during the etching of the cantilevers and releasing these from the handle wafer. Fabrication of the cantilevers was started by the application and patterning of the photoresist mask for

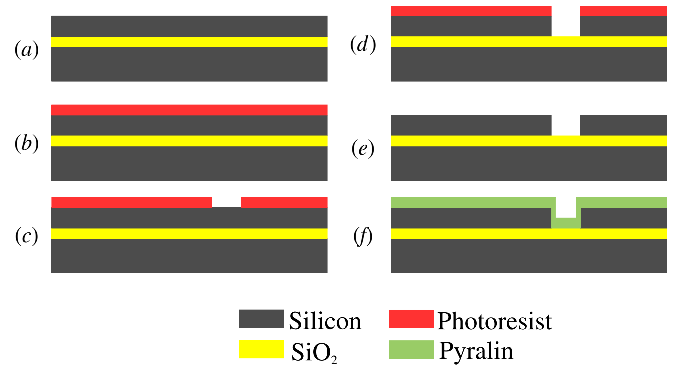

Figure 1. Outline of the fabrication process to obtain cantilevers on the front side of the wafers. (*a*) SOI wafer, (*b*) application of photoresist on the front side, (*c*) patterning of photoresist, (*d*) DRIE of the silicon device layer, (*e*) photoresist removal, (*f*) application of polyimide pyralin as a protective layer.

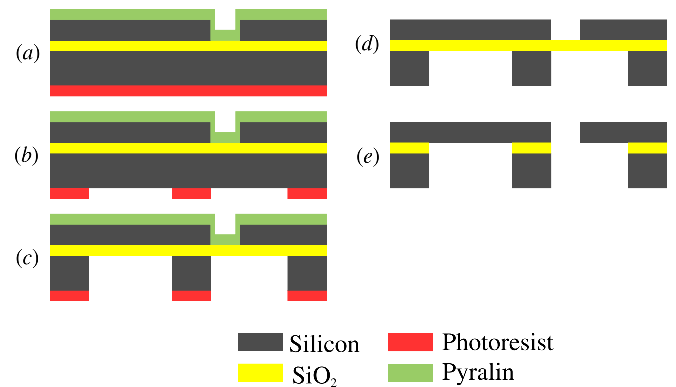

Figure 2. Outline of the fabrication steps on the backside of the wafers for releasing the cantilevers. (*a*) Application of photoresist on the backside, (*b*) patterning of photoresist, (*c*) wafer through DRIE, (*d*) pyralin and photoresist removal from front and backsides, (*e*) etching of the BOX layer using VHF.

defining the cantilevers (*b* and *c*). Subsequently, cantilevers were anisotropically etched by DRIE [28] using SF_6, O_2 and C_4F_8 gases (*d*). After etching of the cantilevers, any remaining photoresist mask material was removed from the front side of the wafers by oxygen plasma (*e*). In the last step of the front side processing of the SOI wafers, polyimide pyralin was spin coated to protect the front side (*f*). In particular, this layer protects the cantilevers from damage during the backside processing of the wafers [29].

Subsequently, cantilevers were released from the handle wafer by making through holes from the backside of the wafers according to the steps shown in figure 2. Starting with the application and patterning of the photoresist on the backside of wafers for defining the holes (*a* and *b*), the backside of wafers was etched by DRIE [28] using SF_6, O_2 and CHF_3 gases (*c*). Subsequently, polyimide pyralin from the front side and photoresist material from the backside of wafers were removed by oxygen plasma (*d*). Finally, the cantilevers were released by etching of the BOX layer using vapors of hydrofluoric acid (VHF) [30] (*e*). The vapor HF etching was stopped after an estimated isotropic etch length of 500 nm. To measure resonance frequencies of the cantilevers in the

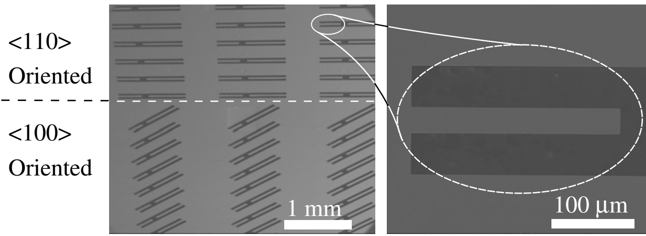

Figure 3. Scanning electron micrographs of the fabricated cantilevers. The cantilevers vary in length from 250 μm to 350 μm in steps of 10 μm. The width and thickness of cantilevers are 30 μm and 3 μm , respectively. The cantilevers are aligned parallel to the ⟨1 1 0⟩ and ⟨1 0 0⟩ crystal orientations of the silicon wafer.

Table 1. PLD parameters for achieving the required deposition conditions.

Parameters	YSZ	SRO	PZT
O_2 pressure (mbar)	0.021	0.13	0.1
Ar pressure (mbar)	0.020	–	–
Temperature (°C)	800	600	600
Fluence (J cm^{-2})	2.1	2.5	3.5
Area of ablation spot (mm^2)	3.35	1.9	3

⟨1 1 0⟩ and ⟨1 0 0⟩ crystal directions of silicon, cantilevers were fabricated aligned parallel to the primary flat of wafers, which corresponds to the ⟨1 1 0⟩ crystal direction of the silicon. For the ⟨1 0 0⟩ crystal direction of the silicon crystal lattice, cantilevers were rotated 45° with respect to the primary flat of wafers. The obtained cantilevers were characterized and inspected by scanning electron and optical microscopy, see figure 3.

3.2. Deposition of PZT by PLD

Deposition of PZT material on the front side of wafers started with depositing 10 nm thick buffer layers of yttria-stabilized zirconia (YSZ) and of strontium ruthenate (SRO) by PLD. These layers act as a barrier against lead diffusion during PZT film deposition and prevent the formation of an excessive SiO_2 amorphous layer on the surface of the silicon substrate. Moreover, these layers also act as a crystallization template for the PZT epitaxial layer growth. After the deposition of buffer layers, 100 nm thick PZT film was deposited by PLD. The PLD parameters with which epitaxial growth of PZT was achieved are listed in table 1 [13]. These PLD parameters, and the use of buffer layers, ensured the epitaxial growth of PZT which is confirmed by phi-scan plots from x-ray diffraction (XRD) [13].

4. Experimental details

4.1. Resonance frequency measurements

The resonance frequency of the cantilevers was measured using thermally excited vibration under ambient conditions by using an MSA-400 micro system analyzer scanning laser-Doppler vibrometer. The free resonance frequency was calculated by curve fitting with the theoretical expression for a second-order mass–spring system with damping.

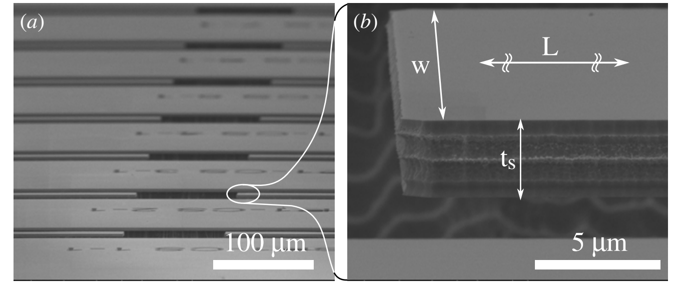

Figure 4. Scanning electron micrograph of cantilevers with applied tilt for non-destructive thickness measurement. (*a*) Wafer tilted in the SEM to locate a particular cantilever. (*b*) Close-up image of the individual cantilever tilted at 5° for thickness measurement.

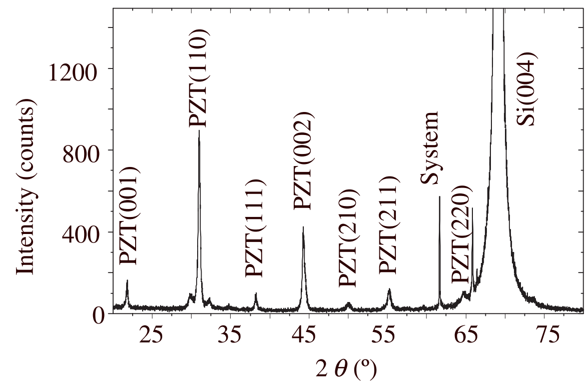

Figure 5. Measured XRD pattern of pulsed laser deposited $PbZr_{0.52}Ti_{0.48}O_3$. The (1 1 0) is the predominant orientation of the deposited PZT.

4.2. Thickness of cantilevers

Uncertainty in the thickness of cantilevers makes the calculation for the effective Young's modulus of PZT unreliable. The supplier of the SOI wafers specifies an error of ± 0.5 μm for the thickness of the device layer, which is 17% uncertainty in the 3 μm device layer. In order to determine the thickness of the individual cantilevers with higher precision, we measured each cantilever by high-resolution scanning electron microscopy. We found that there is a 4% difference in the thickness of the first and last cantilevers, which are 10 mm apart from each other, see figure 4(*a*). The thickness measurement was corrected for the applied tilt as shown in figure 4(*b*) to obtain the final value of the thickness. The cumulative error in the thickness measurement of individual cantilevers was found to be ± 2.2%.

4.3. XRD measurements

In order to reveal the crystal structure and the epitaxial growth of the PZT, XRD measurements were performed. The θ–2θ scan of figure 5 clearly indicates the growth of the PZT thin film with a (1 1 0) preferred orientation. The epitaxial growth of our PZT films can be confirmed by phi-scan plots from the similar samples, reported previously by the authors in [9, 13].

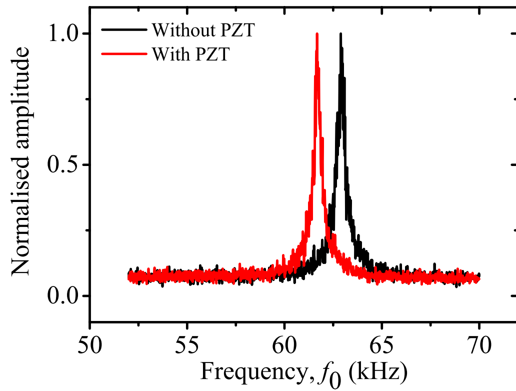

Figure 6. The measured resonance frequency before and after deposition of PZT. The amplitude is normalized to the maximum value. The resonance frequency with PZT is lower than that for the cantilevers without PZT, which is as expected.

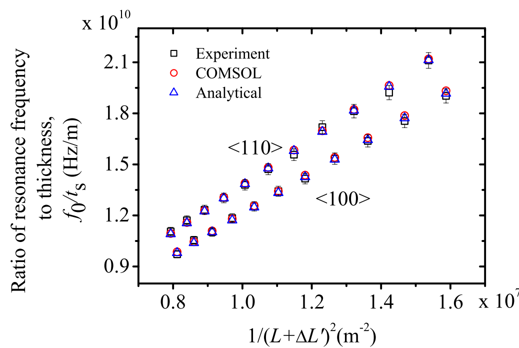

Figure 7. Analytically calculated, simulated and measured resonance frequencies shown as f_0/t_s for cantilevers of varying length. The cantilevers are aligned parallel to the ⟨1 1 0⟩ and ⟨1 0 0⟩ crystal directions of silicon.

4.4. PZT measurements

The second measurement of the cantilever resonance frequency was performed after the deposition of PZT. The difference in the fundamental resonance frequency of a cantilever of length around 250 μm, width around 30 μm, and thickness around 3 μm measured both before and after the deposition of the 100 nm PZT thin film is shown in figure 6. Due to the addition of the PZT thin film on the cantilevers, the resonance frequency was decreased as expected.

5. Discussion

In [21] we have shown that FE simulations validate the use of the Young's modulus E instead of the plate modulus $E/(1-\nu^2)$ as the effective Young's modulus for analytical relation of the resonance frequency for our cantilever dimensions. The ratio of the resonance frequency to the cantilever thickness was plotted against $(L + \Delta L')^{-2}$ in figure 7. The analytical, FE (COMSOL) and experimental results are shown in the plot for easy comparison. The experimentally measured values agree well with the analytically calculated values, which confirms that Young's modulus without a factor of $(1 - \nu^2)$ in the denominator is the appropriate effective Young's modulus

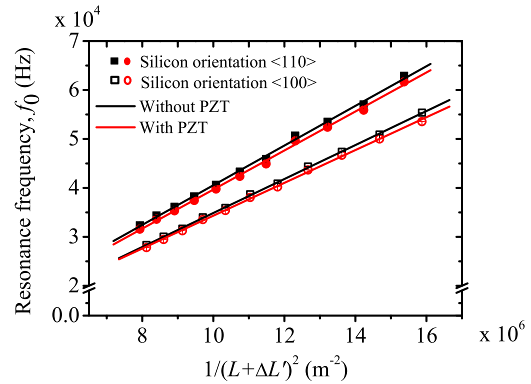

Figure 8. Fundamental resonance frequency versus inverse of effective length squared of the cantilevers, follows a straight line in both the ⟨1 1 0⟩ and ⟨1 0 0⟩ crystal orientation of silicon.

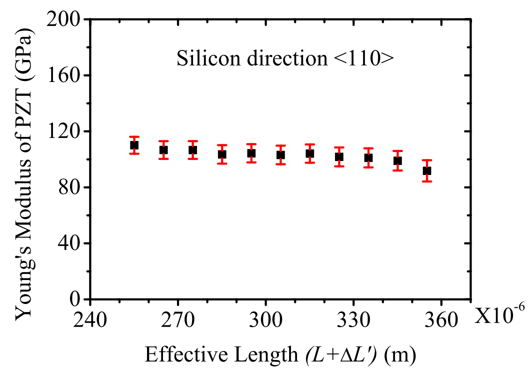

Figure 9. Young's modulus of PZT, calculated for individual cantilevers oriented in the ⟨1 1 0⟩ crystal direction of silicon along with respective error bars. The mean value was determined to be 103.0 GPa with a standard error of ±1.4 GPa.

for our cantilever dimensions. The agreement between FE and the analytical approximation is particularly good for the ⟨1 1 0⟩ silicon direction. A small deviation is found for the ⟨1 0 0⟩ direction.

According to equation (1), the fundamental resonance frequency has a linear relation with inverse of the cantilever length squared. From figure 8, we see that this linear relation is maintained for experimental results of our ⟨1 1 0⟩ and ⟨1 0 0⟩ oriented cantilevers when using the effective length $(L + \Delta L')$ of these cantilevers. The difference in the fundamental resonance frequency of cantilevers before and after the deposition of the PZT thin film is also clear from figure 8.

The Young's modulus of PZT, calculated from equation (2) by using the measured change in the resonance frequency, was found to be 103 GPa with a standard error of ± 1.4 GPa, see figure 9. This value is obtained from cantilevers of varying length aligned parallel to the ⟨1 1 0⟩ crystal direction of silicon. The value for the cantilevers aligned parallel to the ⟨1 0 0⟩ crystal direction of silicon was found to be 95.2 GPa, with a standard error of ± 2.0 GPa, see figure 10. No significant influence of the cantilever length was observed in the Young's modulus of the PZT thin film, as expected. The value of the Young's modulus of the PZT thin film deposited by the PLD is in the same order as values quoted in the

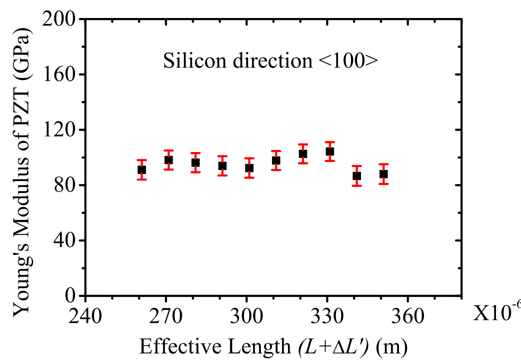

Figure 10. Young's modulus of PZT calculated for individual cantilevers oriented in the ⟨1 0 0⟩ crystal direction of silicon along with respective error bars. The mean value was determined to be 95.2 GPa with a standard error of ± 2.0 GPa.

Table 2. Error analysis for Young's modulus of PZT. Results of a 250 μm long cantilever are used as an example. The error in the t_f is the largest and has the maximum contribution to the cumulative error.

Parameters	Error in parameter (%)	Error in Young's modulus (%)
L	0.5	0.6
t_s	2.2	0.2
t_f	10	5.2
ρ_f	1	1.6

literature such as 25 GPa for sol–gel [31] and 109 GPa for sputter deposited [8] PZT.

A thorough error analysis was performed to calculate the propagation of errors in the parameters to the calculated values for the effective Young's modulus using equation (3). The cumulative error found in the calculated value of the effective Young's modulus is in the order of 6 to 8 GPa for individual cantilevers. Uncertainty about the thickness of the PZT thin film was found as the dominant source of error, as is shown in table 2.

6. Conclusion

We determined the Young's modulus of PLD deposited epitaxial PZT thin films using the resonance frequencies of a range of cantilevers, measured both before and after deposition. From the shift in the resonance frequency of the cantilevers and taking into account their effective undercut length, the thickness of the individual cantilevers and applying a rigorous error analysis, we successfully determined that the in-plane Young's modulus of PZT thin films is anisotropic. The measured Young's modulus of the PZT thin film is 103.0 GPa with a standard error of ± 1.4 GPa for the ⟨1 1 0⟩ crystal direction of silicon and 95.2 GPa with a standard error of ± 2 GPa for the ⟨1 0 0⟩ silicon direction.

The value and anisotropy of Young's modulus is of major importance for the design of MEMS sensors and actuators based on this advanced PLD PZT material. Furthermore, the high-accuracy method of determining Young's modulus of thin films in different in-plane crystal directions of silicon we describe here is generally applicable to any thin film that can be deposited on silicon cantilevers.

Acknowledgments

The authors gratefully acknowledge the support of the SmartMix Program (SmartPie) of the Netherlands Ministry of Economic Affairs and the Netherlands Ministry of Education, Culture and Science. The authors also thank M J de Boer for etching, R G P Sanders for laser-Doppler vibrometer measurements, J G M Sanderink for assistance with SEM, and N R Tas for helpful discussions.

References

[1] Murata M *et al* 2009 High-resolution piezo inkjet printhead fabricated by three dimensional electrical connection method using through glass via *Proc. 22nd IEEE Int. Conf. on Micro Electromechanical Systems (MEMS 2009) (Sorrento, Italy)* pp 507–10

[2] Bronson J R, Pulskamp J S, Polcawich R G, Kroninger C M and Wetzel E D 2009 PZT MEMS actuated flapping wings for insect-inspired robotics *Proc. 22nd IEEE Int. Conf. on Micro Electromechanical Systems, (MEMS 2009) (Sorrento, Italy)* pp 1047–50

[3] Lee J H, Yoon K H, Hwang K S, Park J, Ahn S and Kim T S 2004 *Biosens. Bioelectron.* **20** 269–75

[4] Nam H J, Kim Y S, Lee C S, Jin W H, Jang S S, Cho I J, Bu J U, Choi W B and Choi S W 2007 *Sensors Actuators* A **134** 329–33

[5] Delobelle P, Guillon O, Fribourg-Blanc E, Soyer C, Cattan E and Rèmiens D 2004 *Appl. Phys. Lett.* **85** 5185–7

[6] Deshpande M and Saggere L 2007 *Sensors Actuators* A **135** 690–9

[7] Ledermann N, Muralt P, Baborowski J, Forster M and Pellaux J P 2004 *J. Micromech. Microeng.* **14** 1650–8

[8] Fang T H, Jian S R and Chuu D S 2003 *J. Phys.: Condens. Matter* **15** 5253–9

[9] Dekkers M, Nguyen M D, Steenwelle R, te Riele P M, Blank D H A and Rijnders G 2009 *Appl. Phys. Lett.* **95** 012902

[10] Isarakorn D, Sambri A, Janphuang P, Briand D, Gariglio S, Triscone J M, Guy F, Reiner J W, Ahn C H and de Rooij N F 2010 *J. Micromech. Microeng.* **20** 055008

[11] Ræder H, Tyholdt F, Booij W, Calame F, Østbø N P, Bredesen R, Prume K, Rijnders G and Muralt P 2007 *J. Electroceram.* **19** 357–62

[12] Schweitz J A 1991 *J. Micromech. Microeng.* **1** 10–15

[13] Nguyen M D, Nazeer H, Karakaya K, Pham S V, Steenwelle R, Dekkers M, Abelmann L, Blank D H A and Rijnders G 2010 *J. Micromech. Microeng.* **20** 085022

[14] Finot E, Passian A and Thundat T 2008 *Sensors* **8** 3497–541

[15] Wang Q M and Cross L E 1998 *Ferroelectrics* **215** 187–213

[16] Rúa A, Fernández F E, Cabrera R and Sepúlveda N 2009 *J. Appl. Phys.* **105** 113504

[17] Van Kampen R P and Wolffenbuttel R F 1998 *Sensors Actuators* A **64** 137–50

[18] Matin M A, Akai D, Kawazu N, Hanebuchi M, Sawada K and Ishida M 2010 *Comput. Mater. Sci.* **48** 349–59

[19] Babaei Gavan K, van der Drift E W J M, Venstra W J, Zuiddam M R and van der Zant H S J 2009 *J. Micromech. Microeng.* **19** 035003

[20] Cleland A N, Pophristic M and Ferguson I 2001 *Appl. Phys. Lett.* **79** 2070–2

[21] Nazeer H, Woldering L A, Abelmann L, Nguyen M D, Rijnders G and Elwenspoek M C 2011 Influence of silicon orientation and cantilever undercut on the determination of the Young's modulus of thin films *Microelectron. Eng.* at press (doi:10.1016/j.mee.2011.01.028)

[22] Volterra E and Zachmanoglou E C 1965 *Dynamics of Vibrations* (Columbus, OH: CE Merrill Books)

[23] Deslattes R D, Henins A, Bowman H A, Schoonover R M, Carroll C L, Barnes I L, Machlan L A, Moore L J and Shields W R 1974 *Phys. Rev. Lett.* **33** 463–6

[24] Rasmussen P A 2003 Cantilever-based sensors for surface stress measurements *PhD Thesis* Technical University of Denmark

[25] Brantley W A 1973 *J. Appl. Phys.* **44** 534–5

[26] Gere J M 2006 *Mechanics of Materials* (Toronto: Thomson-Engineering)

[27] Taylor J R 1997 *An Introduction to Error Analysis: The Study of Uncertainties in Physical Measurements* (Sausalito, CA: University Science Books)

[28] Jansen H V, de Boer M J, Unnikrishnan S, Louwerse M C and Elwenspoek M C 2009 *J. Micromech. Microeng.* **19** 033001

[29] Loh N C, Schmidt M A and Manalis S R 2002 *J. Microelectromech. Syst.* **11** 182–7

[30] Anguita J and Briones F 1998 *Sensors Actuators* A **64** 247–51

[31] Piekarski B, DeVoe D, Dubey M, Kaul R and Conrad J 2001 *Sensors Actuators* A **91** 313–20